ADVANCED MATERIALS

DOI: 10.1002/adma.200601443

Forced Soft Lithography (FSL): Production of Micro- and Nanostructures in Thin Freestanding Sheets of Chitosan Biopolymer**

By *Javier G. Fernandez*, *Christopher A. Mills*,* *Mateu Pla-Roca*, and *Josep Samitier*

Biopolymers are increasingly being studied with respect to cell-surface interactions. Polymers are advantageous for these studies because they are largely biocompatible and can be used to produce a number of micro- or nanostructured replicas cheaply. The biomedical applications of these polymers include tissue engineering[1,2] and biomedical implants.[3] In such applications, the surface topography of the polymer plays an important role in the well-being of the growing cells.[4] As it may also be possible to control the characteristics of the cell using structured surfaces,[5] the development of techniques for micro- and nanostructuring biopolymers is becoming increasingly important.

A broad range of methods are available to control surface topography. Nanoembossing (NE)[6] and soft lithography (SL)[7] are increasingly common techniques for producing structured polymer surfaces. Although both techniques have numerous advantages, they do have some drawbacks. NE takes place at temperatures which can be detrimental to delicate, bio-functionalized polymers, and is limited to using solid state, thin films of thermoplastic polymers, which are typically spun down onto inorganic substrates. SL, on the other hand, is only suitable for elastomeric (liquid) pre-polymers and the choice of polymer-mould combinations can be limited, as we shall demonstrate.

Forced Soft Lithography: We have used FSL for the faithful production of micro- and nanostrucutred polymer replicas using the solution-processable biopolymer, Chitosan. Figure 1 presents a schematic diagram showing the steps involved in FSL. The mould is placed in the bottom of a poly(propylene)

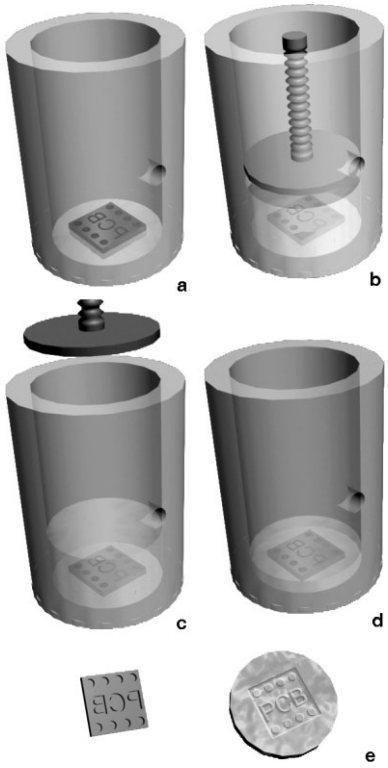

Figure 1. Schematic diagram of the Forced Soft Lithography technique. The silicon mould is placed in the press with the structures to be replicated on the upper surface (a). The liquid polymer is poured on the mould and forced to enter the mould cavities under pressure for ~1 minute (b). The pressure is released and the press opened (c) allowing the solvent to evaporate (d). When the polymer is fully cured, the replica is simply pealed off the mould (e).

chamber with the structures to be replicated uppermost (a). The liquid pre-polymer is poured into the chamber before a plunger is inserted and pressure is applied via an external press (b). This compresses the polymer to a pressure of between 2×10^5 and 1×10^6 Pa in ~1 minute. The pressure is re-

[*] Dr. C. A. Mills, J. G. Fernandez, Dr. M. Pla-Roca, Prof. J. Samitier
Laboratory of Nanobioengineering—CIBER-BBN
Institut de bioenginyeria de Catalunya (IBEC)
Barcelona Science Park, C/Josep Samitier 1–5, Barcelona 08028 (Spain)
E-mail: cmills@pcb.ub.es; jgfernandez@pcb.ub.es
J. G. Fernandez, J. Samitier
Department of Electronics, University of Barcelona
c/Martí i Franquès 1, 08028 Barcelona (Spain)

[**] We would like to thank D. Caballero Vila (Parc Cientific de Barcelona) for his help in the production of the AFM images in Figure 4. We also thank X. Sisquella (AFM), M.-J. Lopez Bosque (FIB), E. Martinez (FIB) and A. Errachid (DRIE) from the Parc Cientific de Barcelona for technical assistance with this work, as well as Dr. L. Fumagalli for her comments. Thanks also go to Drs. J. Bausells and G. Villanueva at the Centro Nacional de Microelectronica (Barcelona) for supplying the microstructured moulds used here. This paper and the work it concerns were generated in the context of the Cell-PROM project, funded by the European Community as contract N°. NMP4-CT-2004-500039 and it reflects only the authors' views. Support for this work from the Spanish Ministry for Science and Education through the provision of FPU (J. G. F.) and Ramon y Cajal (C. A. M.) grants is also gratefully acknowledged.

leased and the chamber is opened (c) allowing solvent evaporation to occur and the curing process to begin (d). After curing for 36 h, the polymer is simply pealed off the surface of the mould (e). All the process steps, including the pressurization and the curing/evaporation, are carried out at room temperature.

Polymer and mould preparation and characterisation is detailed in the supporting information. The moulds used for our SL experiments have been indirectly characterized with respect to their shape and dimensions using Poly(methyl methacrylate) (PMMA) NE, and with respect to their surface energy using water contact angle measurements. The average height of the structures, in five PMMA replicas (~600 post structures) of the two moulds used here, was 745 nm and 400 nm. The surface area of the structures in each case was $5 \times 5\ \mu m^2$. Contact angle measurements on the non-functionalized silicon nitride (Si_3N_4) moulds revealed an advancing H_2O contact angle of 83.7°, which agrees with previously reported values.[8] Upon functionalization to produce a (hydrophilic) mould with a high surface energy, the advancing H_2O contact angle decreased to 66.7°. When the Si_3N_4 was functionalized to produce a (hydrophobic) mould with a low surface energy, the advancing H_2O contact angle increased to 130.0°.

Polymer Replication: Conventional SL operates by filling the entirety of the mould by the liquid pre-polymer in order to form a negative replica of the mould. This is commonly achieved at room temperature and with no applied pressure. Under these conditions, for the production of structures at the micron and sub-micron range, the force due to gravity is negligible and capillarity forces dominate.[9] Filling of the mould depends on the polymer displacing the air in the mould cavities. The displacement process therefore requires that a critical pressure is achieved. This is described empirically by Tenan et al.[10] and is theoretically explained as the difference in energy of the cavity when it is filled with air compared to when it is filled with polymer. If this pressure is not reached the polymer will only be able to enter the cavity to the point at which the capillarity force balances the opposing force realized by the compressed air.

The pressure required to displace the air depends on an affinity factor related to the nature of the gas in the cavity (air in this case), on the polymer employed, and also on the mould material. We have undertaken chemical functionalization of the surface of the mould to introduce variation in the mould surface energy. If the surface energy of the mould is high, the attractive (adhesion) forces between the mould surface and the liquid pre-polymer are strong. These adhesion forces overcome the surface tension in the polymer, and allow it to fill the cavity. As the surface energy decreases, the adhesion forces are minimized, making it hard for the polymer to enter the mould cavity. Consequently the pressure applied by the polymer on the air in the cavity is minimized and the air is not displaced.

The pressure necessary to move the bubble of air is also inversely dependent on the dimensions of the cavity to be filled. Moulds with arrays of point-like cavities were chosen because of the difficulty of replicating post-like structures in polymers using conventional replication methods. Moulds which produce line or cavity structures in the polymer require less forceful replication conditions. We have therefore chosen the worst chemical and geometrical conditions for the replication process in order to demonstrate the capabilities of the FSL method.

Figures 2 and 3 compare SL and FSL for PDMS and Chitosan respectively using high surface energy and low surface energy functionalized moulds. In each case, the figures show a histogram of the heights of the points measured from a $125 \times 95\ \mu m^2$ white light interferometry image of the polymer replica, which contains ~120 post-like structures. The *y*-axis data have been normalized. The first peak in each histogram constitutes those points at the base of the polymer replica. In each case this value has been adjusted to 0 on the *x*-axis. The second peak in each histogram constitutes those points at the top of the post-like structures. Inset in each figure are sectional profiles of a small number of the replicated structures for comparison of their shapes.

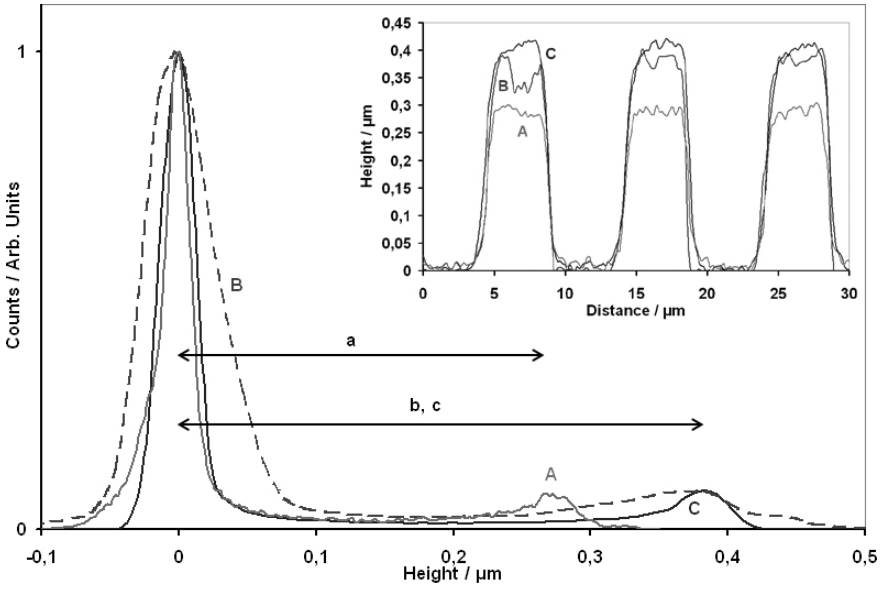

Figure 2. Graph of the normalized distribution of heights of PDMS posts ($5 \times 5\ \mu m^2$) in a $125 \times 95\ \mu m^2$ area of a white light interferometry image. The posts are produced using conventional SL using low (A) and a high (B) surface energy moulds, and using FSL with a low surface energy mould (C). The average heights of the posts in each case is $a = 267$ nm and b, $c = 385$ nm. Inset are 30 µm long cross sectional profiles of the posts produced using each of the techniques.

ADVANCED MATERIALS

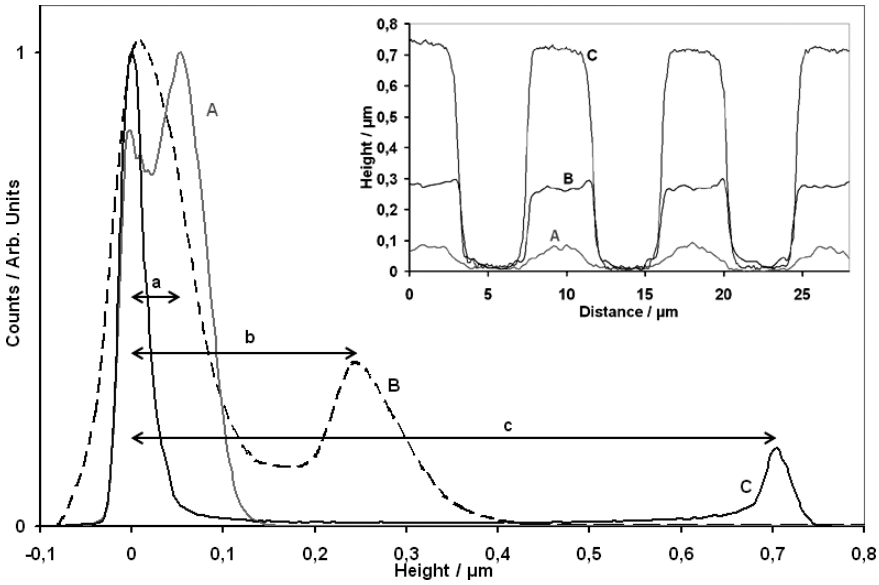

Figure 3. Graph of the normalized distribution of heights of Chitosan posts ($5 \times 5\ \mu m^2$) in a $125 \times 95\ \mu m^2$ area of a white light interferometry image. The posts are produced using conventional SL using low (A) and a high (B) surface energy moulds, and using FSL with a low surface energy mould (C). The average heights of the posts in each case is $a = 55$ nm, $b = 201$ nm, and $c = 710$ nm. Inset are 28 µm long cross sectional profiles of the posts produced using each of the techniques.

When using Chitosan, the results are even more dramatic. If conventional SL is undertaken using a non-optimal polymer/mould combination, i.e., Chitosan and a low surface energy mould, the replicated structures are only ~55 nm tall (A in Fig. 3). If the mould is functionalized to increase its surface energy (B in Fig. 3) the height of the posts quadruples to ~201 nm tall. However, as the mould cavities are 745 nm deep, the mould filling is incomplete in each case, with, respectively, less than 8 % and 27 % of the mould filled. This highlights the problem of using non-optimal polymer/mould combinations when attempting to produce microstructures in a non-elastomeric polymer using SL. Using FSL with the low energy mould surface and with an applied pressure of 4×10^5 Pa, the height of the structures increases to 710 nm, filling ~95 % of the total volume (C in Fig. 3). This is probably the best result achievable with this method because the polymer will shrink slightly during the solvent evaporation/curing process.

In the case of PDMS (Fig. 2), using a 400 nm deep mould with a low surface energy and without any kind of external force, the polymer produces replica structures up to 267 nm tall (68 % of the expected height) (A in Fig. 2). The replicated structures have similar heights whether they are cured at 80 °C for 1 hour or at room temperature for 24 h. The complete filling of the mould in this case can be achieved by one of two methods. The mould can either be chemically modified to produce a high energy mould surface, which increases the adhesive forces between the PDMS and the mould surface and causes almost complete filling (~96 %) of the mould cavities (B in Fig. 2), or FSL can be used to force the polymer to enter the mould cavities, even when the mould has a low energy surface (C in Fig. 2). This shows that the type of mould material used is important when considering implementing SL. However, even with a bad polymer/mould combination, FSL can be used to overcome the forces which lead to incomplete filling of the mould cavities.

The quality of the replicas is also improved in FSL, compared to SL replicas produced using the optimized mould. The full width at half maximum (FWHM) of the peaks represents the height distribution (roughness) of the surfaces of the polymer. The FWHM of the upper surface of the FSL replicas (peak 2) is smaller than for the SL replicas, suggesting that the roughness is lower for the FSL replicas. This characteristic can also be qualitatively observed in the profile of the peaks (Inset in Fig. 2) where the top surface of the replicated PDMS structures produced using FSL using the chemically modified mould (C) are flatter than those produced by SL (B).

The pressure required to remove air present in the cavities will increase as the cavity size decreases. Therefore externally forcing the polymer into a nanometric dimensioned mould will be more important than for a micrometric mould. Experiments using a nanometric mould, containing lines ~200 nm wide and 100 nm deep (Fig. 4a), reveal that curing the Chitosan without applying any pressure produces replicated structures up to 73 % of the expected height. This result is higher than expected, but may be explained due to the shape of the structures in the focused ion beam (FIB) fabricated mould. The Gaussian beam shape of the FIB makes it difficult to produce mould cavities with vertical side-walls. The cavities in the mould are therefore Gaussian in shape, which are easier

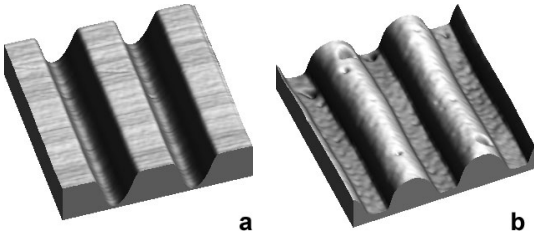

Figure 4. AFM images of a) a low surface energy mould nanostructured using FIB, and b) a Chitosan replica produced from this mould using FSL. Scan area in each case = $2 \times 2\ \mu m^2$. Comparison of the average height of the nanostructures produced using SL and FSL, with the depth of the structures in the mould, reveals an increase in average structural height of 21 % using FSL

to fill with polymer than a cavity with vertical side-walls. Even so, when using FSL, with an applied pressure of 4×10^5 Pa, the average height of the structures in the replica (Fig. 4b) increases to 94 % of the expected height.

It is possible to increase the adhesion forces between the mould and the polymer by altering the properties of the pre-polymer. For example, adding less cross-linking agent when preparing PDMS can be used to produce a low viscosity, "sticky" polymer which will enter the mould cavities more easily. This however has the effect of altering the properties of the final SL polymer replica. Reducing the amount of cross-linking agent causes the PDMS replica to have a lower Young's modulus and hence it is more flexible. In some cases, it may be necessary to use a combination of polymer and mould which is not ideal to produce a polymer replica with the required physical or chemical properties, and for this FSL is a useful technique.

Replica Transparency: The transparency of the replicas was also studied. A Chitosan replica formed by simple vacuum degassing of the liquid pre-polymer was compared with one produced by FSL. In the former case the polymer-mould system was introduced into a vacuum chamber at 1.8×10^4 Pa for 1 minute; equivalent to the time used to apply the pressure in FSL. Both samples were cured for the same amount of time and peeled off the mould before being examined in the visible range of the electromagnetic system using an ultra-violet/visible spectrometer (UV1240 UV-vis spectrometer, Shimadzu Corp., Japan). The transparency of the FSL replica increased from 82 % at 350 nm to 98 % at 800 nm, whereas the transparency of the vacuum prepared replica increased from 66 % to 82 %. This approximately corresponds to a 20 % greater transparency in the FSL produced sample across the measurement range. This agrees with previously reported results for PDMS at higher temperatures.[11]

Mould Filling: The filling of the mould and possible bubble formation can be examined theoretically. When two phases come into contact, an interfacial tension appears and can be described as the balance between the two surfaces tensions, Γ_{XY}, less an energy lowering associated with attractive forces between the molecules of the two phases. When a liquid is in contact with a solid and a gas (a three phase system), at equilibrium, the chemical potential in the three phases should be equal. The surface contact will change, via a change in the liquid-solid contact angle, $0° < \theta < 180°$, until this equilibrium is reached. If $\theta < 90°$ the solid–liquid interface is of lower energy than the solid–gas interface and within a capillary, a phenomenon called "capillary rise" is expected to occur.[12] This phenomenon consists of the the liquid rising along the capillary in order to seek a lower interfacial energy state.

In our experiments at the micro- and nanoscale, the action of gravity is negligible and capillarity will be the main force involved in the process. Through application of an external force, equilibrium is reached when the pressure due to the external force, P_{ext}, plus the pressure due to capillarity, P_{cap}, equals the pressure of the compressed air in the closed cavity,

$$P_{air} = P_{cap} + P_{ext} \tag{1}$$

If we assume that the gas is ideal and that, prior the entrance of the polymer (initial state), it is at atmospheric pressure (P_{atm}), we can apply Boyle's law to calculate the change in pressure due to the change in volume of the trapped air. The height of the liquid column under these conditions is given by,

$$\xi = D\left(1 - \frac{P_{atm}a}{2\gamma_L \cos\theta + P_{ext}a}\right) \tag{2}$$

where a and D are the radius and the depth of the cavity respectively and γ_L is the liquid polymer surface tension assuming that, generally, $\gamma_L \approx \gamma_{LG}$ (the polymer/gas interfacial tension).

Equation 2 models the entrance of the polymer, in its liquid state, into the cavities of the mould, both for those techniques employing an external force (FSL) and for those where only capillarity is responsible for polymer replication (SL), in the latter case $P_{ext} = 0$. The equation assumes air in the mould is not displaced and states that there are two ways to increase the quality of the structures (i.e., increase ξ). Firstly, we can decrease the contact angle between the polymer and the surface. As γ_L is constant, and characteristic of the polymer, the contact angle can be decreased by increasing the surface energy of the mould (i.e., by chemical functionalisation of the mould surface). Secondly, we can increase P_{ext}: this is the basis of the FSL technique.

From Equation 2 we can obtain the maximum height of the structures it is possible to produce by chemical modification of the mould alone. In the ideal condition where the minimum contact angle is 0°, the maximum height achievable is,

$$\xi(0°) = D\left(1 - \frac{P_{atm}a}{2\gamma_L}\right) \tag{3}$$

if the air is not displaced from the mould cavities. Therefore, the height of the replicated structures, created by varying the contact angle, has a theoretical limit. However, when additional external pressure is applied, the height of the structures is only limited by the mould dimensions. Equation 2 also reveals the maximum value of the contact angle that the polymer must possess in order to produce a replica of the mould using ambient experimental conditions. The limit is obtained when $\xi = 0$ and is given as,

$$\cos\theta_{max} = \frac{P_{atm}.a}{2\gamma_L} \tag{4}$$

A polymer with a contact angle, on the surface of the mould, larger than that presented in Equation 4 will not form complete structures if neither chemical modification nor ex-

ADVANCED MATERIALS

ternal force is employed. Note that these equations are valid at micro- and nanoscales only. At larger scales, effects due to gravity become significant when modelling the filling of the mould by the polymer.

Air Bubble Removal: In the above theroretical description, the effects of an external pressure are described and a constant volume of air in the mould is assumed. However, the results for FSL (where the replicas faithfully replicate the mould and the transparency is high) show that, during the application of the external pressure the air is removed from the cavities. If the air was just compressed, after the retraction of the piston, the air would return to its original volume and would affect the quality of the final replica. Instead, small gas bubbles are detached from the mould surface by the change in volume of the polymer under a high pressure: they are then driven out of the bulk of the polymer by the drag force acting on the bubble. In the case of larger bubbles, the compression is not enough to free a bubble and mass transport through the bubble-polymer interface is the main process for bubble elimination.

The presence of bubbles on the mould surface can originate through three processes: nucleation by super-saturation within the mould cavities (classical nucleation theory), the entrapment of air during polymer pouring[13] or the capture of travelling bubbles by the cavities.[14] Here, the capture of travelling bubbles can be neglected because we assume that the polymers employed are entirely degassed before pouring on the mould; PDMS is degassed in a vacuum chamber and Chitosan during centrifugation.

To discover whether the initial formation of the bubble comes from a Harvey nucleus (a pre-existing gas providing a stable source for nucleation) formed due the entrapment of air in the master cavities during the pouring process, or whether it is nucleated directly in the cavities is not the aim of this paper, we require only to describe why bubbles are not present in the final replicas. We will, however, describe the general case of nucleation due to the change in the super-saturation conditions, taking into account that, in both the cases mentioned above, bubble growth is a thermodynamically favourable process within the mould cavities.

One condition necessary for bubble nucleation is the super-saturation of the polymer, a condition fulfilled if the vapour pressure exceeds the pressure in the bubble, i.e., $P_{atm} > P_{ext}$. When the system is super-saturated the free energy associated with transferring gas molecules to the new phase (the bubble nucleation site) is negative and hence thermodynamically favourable. A common example of this is "decompression sickness" in scuba diving. If the diver has surfaced too quickly, nitrogen in the blood, a component of the compressed air in their tanks, super-saturates and bubbles form in the blood stream which can interrupt blood flow. This is remedied by transferring the diver to a pressurised container. Within the container, the gas pressure is high, which causes the nitrogen bubbles to be destroyed. A step by step decompression is then undertaken to allow the dissolved nitrogen gas to be expelled naturally, without allowing super-saturation to re-occur.

At a molecular level, the mass transport through the bubble surface can be calculated from Fick's law in terms of the diffusion coefficient of the gas phase (D), which can be rewritten in terms of the pressure on the system by employing Henry's law,

$$\dot{M} = \sqrt{\frac{D}{\pi t}}(P_{atm} - P_{ext})\frac{A}{H} \quad (5)$$

where t is time, A the free surface, and H is a constant. The initial equilibrium gas (air) pressure used is atmospheric pressure P_{atm} because this is the pressure at which the polymer is stored and at which the bubble has been formed. A negative value of $\dot{M}$ will mean mass transport from the bubble to the liquid. An increase in the external pressure will hence cause the bubble to decrease in size, as the air redissolves into the bulk polymer, until it is destroyed or detaches from the surface. The diffusion rate is proportional to the absolute value of the pressure difference, i.e., the higher the external pressure is, the faster the air is removed.

Reduction in the external pressure will cause air transport from the polymer into a bubble with the consequent increase in bubble size. Some bubbles then will grow until they reach the critical radius (when the drag force equals the bubble-surface coupling force) and eventually they will detach from the surface, in those cases the bubble may leave behind a portion of adsorbed gas that will again act as a Harvey nuclei[15] promoting the grow of a new bubble. All the bubbles that do not reach the critical radius will remain in the mould cavities and hence will degrade the quality of the polymer replica.

However, utilising too high a pressure can cause super-saturation to re-occur after removal of the pressure, and hence the possibility of bubbles nucleating again. Equation 5 suggests that, after the release of the external pressure, the mass transport through the bubble interface will change direction and some bubbles would grow. In FSL however, the system is initially under positive external pressure (a negative super-saturation) long enough to remove the air in the mould cavities, and no Harvey nuclei remain to initiate bubble nucleation. In this case only classical nucleation events are possible, a process which requires very high levels of super-saturation (tens of magnitude higher than possible here) because of the need to overcome the energy barrier due to the production of a considerable interfacial free energy. Therefore, when the pressure is removed no bubbles will form at the mould surface.

During a decompression of the polymer, structures in the mould surface act as nucleation sites for the formation of bubbles, responsible for the lower transparency in the replica produced by vacuum degassing. Vacuum decompression is a good process for the elimination of air dissolved in the bulk of the liquid pre-polymer but, if carried out in the presence of the mould, it leads to the nucleation of bubbles at the mould surface. For an excellent review on bubble nucleation and growth, refer to Jones.[15]

In summary, FSL has been developed for the micro and nanostructuring of solution processable polymers, for experiments where the polymer/mould compatibility is not ideal for

conventional SL. The technique has been shown to be useful when attempting to structure Chitosan biopolymer at the micro- and nanoscale, especially as altering the chemical properties of the mould (e.g., to change the hydrophobicity) does not facilitate complete Chitosan structural replication via conventional SL techniques. FSL may be particularly useful when attempting to structure delicate, biocompatible or biofunctionalised polymers because no elevated temperatures are required (the replication takes place at room temperature) and the pressures applied are relatively low ($< 1 \times 10^6$ Pa). The technique is inherently designed to avoid bubble formation in the replicas leaving them with excellent transparency.

Such structured, freestanding polymer sheets have a number of advantages when it comes to their use in biomedical applications. For example, bio-incompatible inorganic substrates that could affect cell culture are not present, and the polymer can easily be cut to the required shape for use with existing cell culture apparatus, e.g., culture plates. Finally, FSL retains all the advantages of conventional SL, including its simplicity, low technology requirements and the possibility of large area replication, while further opening the field of SL by allowing non-optimal polymer/mould combinations to be utilized.

Received: June 29, 2006
Revised: August 2, 2007

[1] G. D. Pins, M. Toner, J. R. Morgan, *FASEB J.* **2000**, *14*, 593.
[2] S. Levenberg, J. Rouwkema, M. Macdonald, E. S. Garfein, D. S. Kohane, D. C. Darland, R. Marini, C. A. van Blitterswijk, R. C. Mulligan, P. A. D'Amore, R. Langer, *Nat. Biotechnol.* **2005**, *23*, 879.
[3] A. D. Martino, M. Sittinger, M. V. Risbud, *Biomaterials* **2005**, *26*, 5983.
[4] A. S. G. Curtis, B. Casey, J. O. Gallagher, D. Pasqui, M. A. Wood, C. D. W. Wilkinson, *Biophys. Chem.* **2001**, *94*, 275.
[5] S. Levenberg, N. F. Huang, E. Lavik, A. B. Rogers, J. Itskovitz-Eldor, R. Langer, *Proc. Natl. Acad. Sci. USA* **2003**, *100*, 12 741.
[6] S. Y. Chou, P. R. Krauss, P. J. Renstrom, *Science* **1996**, *272*, 85.
[7] Y. Xia, G. M. Whitesides, *Angew. Chem. Int. Ed.* **1998**, *37*, 550.
[8] M. Ueda, C. M. Lepienski, E. C. Rangel, N. C. Cruz, F. G. Dias, *Surf. Coat. Technol.* **2002**, *156*, 190.
[9] N. Ichikawa, Y. Satoda, *J. Colloid Interface Sci.* **1994**, *162*, 350.
[10] M. A. Tenan, S. Hackwood, G. Beni, *J. Appl. Phys.* **1982**, *53*, 6687.
[11] D. E. Robinson, A. E. Higinbotham, P. C. Wankat, *Ind. Eng. Chem. Prod. Res. Dev.* **1969**, *8*, 502.
[12] F. W. Sears, M. W. Zemansky, *University Physics*, Addison-Wesley, London, **1964**.
[13] S. G. Bankoff, *AIChE J.* **1958**, *4*, 24.
[14] M. Dennis Desheng, K. Joonwon, K. Chang-Jin, *J. Micromech. Microeng.* **2006**, *16*, 419.
[15] S. F. Jones, G. M. Evans, K. P. Galvin, *Adv. Colloid Interface Sci.* **1999**, *80*, 27.